DOE/MC/3 1384--5280
(DE9601 1380)
Distribution Category UC-103

Analysis And Control Of The METC Fluid Bed Gasifier

Final Report
(Includes Technical Progress Report for October 1994- January 1995)
September 1994- September1996

Work Performed Under Contract No.: DE-FG21-94MC31384

For
U.S. Department of Energy
Office of Fossil Energy
Morgantown Energy Technology Center
P.O. Box 880
Morgantown, West Virginia 26507-0880

By
University of South Carolina
Office of Sponsored Programs and Research
Columbia, South Carolina 29208

September **1996**

Disclaimer

Table of Contents

I. Overview of Work

This document presents a modeling and control study of the Fluid Bed Gasification (FBG) unit at the Morgantown Energy Technology Center (METC). The work is performed under contract no. DE-FG21 -94MC3 1384. The purpose of this study is to generate a simple FBG model from process data, and then use the model to suggest an improved control scheme which will improve operation of the gasifier. The work first developes a simple linear model of the gasifier, then suggests an improved gasifier pressure and MGCR control configuration, and finally suggests the use of a multivariable control strategy for the gasifier.

A successful control scheme for the FBG must operate successfully in both the servo and regulatory modes. In the servo mode, the control system must adjust the reactor input variables so that the reactor output meets operational objectives. A number of objectives must be met on the FBG:

1. No clinkering
2. High carbon conversion
3. Meet targeted gas make
4. Meet targeted bed density
5. High gas heating value
6. Meet targeted Fuel/non combustible mole ratio
7. Meet targeted mean bed temperature
8. Maintain HOC balances and inventories.

In the regulatory mode, the controller must respond to disturbances such as coal moisture content, inlet air or steam temperature, and ambient conditions in an intelligent manner.

Presently all of these objectives and more are considered by operators during gasifier operation, All inlet gas flow rates are flow controlled with simple PID-type controllers, gasifier backpressure is controlled via a split range controller, and MGCR pressure is controlled via a PID controller. The backpressure control is critical to steady operation of the gasifier, as fluctuations in backpressure impact inlet gas flowrates and bed density. More detail on backpressure and MGCR control is given in the next section. Typically the maximum bed temperature is maintained by adjusting the air flow setpoint, gas moisture content is maintained at 10% by adjusting the steam flow setpoint.

II. Linear Model

A linear transfer function based model for the FBG was developed based on the data from Gasifier run 11. The approach was the same as that taken for a transfer function model derived from Gasifier run 10. The methodology is outlined in the technical progress report for the period 10/1/94 to 1/31/95 (see Appendix I).

Table 1 below summarizes the steady-state operating conditions for FBG run 11.

Coal Type	Montana #7
Coal Feed rate	70 lb/hr
Reactor Air flow	1025 scfh
Convey Air	1600 scfh
Steam flow rate	52 lb/hr
Cone Nitrogen flow	0 scfh
Cone Steam	9 lb/hr
Nitrogen Underflow	250 scfh
Operating Pressure	425 psi

Table 1: FBG Run #10 Baseline Operating Condition

Note that during the beginning of the run, 50 scfh of cone Nitrogen was fed instead of cone steam, The switch to cone steam was made part way through the run.

Tables 2 and 3 give the tests that were made during the gasifier run 11. Note that the run covered two time periods, from July 16 to 22, and July 24 to August 8. The data includes changes in reactor air, coal feed rate, underflow N2, reactor steam, switch from cone steam to cone Nitrogen, and switch from Montana #7 coal to coke breeze. The transfer function model derived from FBG run 11 is given in Table 4. It should be recognized that there is a high degree of uncertainty in the model, especially in temperatures (which were averaged).

Test Period (TP#)	Hrs.	Cum. Time***	Start Time	End Time	Coal Type	Coal Feed Rate lb/h	Reactor Air scfh	Convey Air scfb	Reactor Steam lb/h	Cone Steam lb/h	Cone N2 scfb	Cone Flow N2 scfh	Reactor Pressure psig	Test Parameters
	16	16	7/16/95 20:00	7/17/95 11:56		0	5000	0	0	0	50	350	425	Startup
	1.25	17.25	7/17/95 11:56	7/17/95 13:13	Montana #7	30.6	2300+	800-1600	0	0	55	350	425	Combustion/Fl Il Bed
	5.25	22.5	7/17/95 13:13	7/17/95 18:30	#7	70	525-825	1600	56	0	55	350	425	Stabilization
1a	4	26.5	7/17/95 18:30	7/17/95 22:21	#7	70	1025	1600	56	0	50	300	425	Baseline
	6	32.5	7/17/95 22:21	7/18/95 4:30	Lost of coal feed due to feeder plug by foreign material in feed									Hot-Hold
1b	9	41.5	7/18/95 4:30	7/18/95 13:30	#7	70	1025	1600	52	0	50	300	425	Baseline*
2#	12	53.5	7/18/95 13:30	7/19/95 1:30	#7	70	1085	1600	52	0	50	300	425	Reactor Air
3#	12	65.5	7/19/95 1:30	7/19/95 13:30	#7	70	1025	1600	52	0	50	300	425	
4	13.25	78.75	7/19/95 13:30	7/20/95 2:45	#7	70	1025	1600	52	6	0	300	425	Cone N2 to Steam
5	6.75	85.5	7/20/95 2:45	7/20/95 9:32	#7	70	1025	1600	52	6	0	250	425	Baseline
6	16	101.5	7/20/95 9:32	7/21/95 1:30	#7	70	1025	1600	52/66/79		0	250	425	Rx & Cone Steam
7	12.3	113.8	7/21/95 1:30	7/21/95 13:49	#7	80	1025	1600	66	9	0	250	425	Coal
8	12	125.8	7/21/95 13:49	7/22/95 1:40	#7	70	1025	1600	66	9	0	250	425	Feed
9	12.2	138	7/22/95 1:40	7/22/95 13:52	#7	60	1025	1600	66	9	0	250	425	Rate
	6	144	7/22/95 13:52	7/22/95 20:00		0	4200/7000 N2	800 N2	0	0	100	2000	425-0	Cool Down

* Old Baseline (94FBG10). ** New Baseline (95FBG11) *** Total Gasification Time = 115 hours

Sample UF & OF each per hour during the 2nd half of TP#2 and the entire TP#3; total of 19 samples between TP#2 and 3.

Table 2: Test Matrix Completed for 95FBG11 (July 16 to 22, 1995)

Test Period	Hrs.	Cum. Time**	Start Time	End Time	Coal Type	Coal Feed Rate	Reactor Air	Convey Air	Reactor Steam	Cone Steam	Cone N2	Underflow N2	Reactor Pressure	Test Parameters
						lb/h	scfh	scfh	lb/h	lb/h	scfh	scfh	psig	
	22	22	7/24/95 20:00	7/25/95 17:53		0	5000	0	0	0	50	350	425	Startup
	1	23	7/25/95 17:53	7/25/95 18:53	Moolyns #7	30.6	2300+	800-1600	0	0	55	350	425	Combustion
	1	24	7/25/95 18:53	7/25/95 20:00	#7	70	525-825	1600	65	0	55	350	425	Fill bed
	5.75	29.75	7/25/95 20:00	7/26/95 1:45	#7	70	1025	1600	66->52	0	50	300	425	Stabilization
														Baseline
1	5.5	35.25	7/26/95 1:45	7/26/95 7:15	Shut down due to valve malfunction									Shut Down
	12	47.25	7/26/95 7:15	7/26/95 19:13										Combustion
	1	48.25	7/26/95 19:13	7/26/95 20:15	#7	30.6	1025	1600	0	0	55	250	425	Fill Bed
		48.25	7/26/95 20:15		#7	30.6->70	500->1025	1600	60	0	55	250	425	Stabilization
	5.25	53.5		7/27/95 1:30	#7	70	1025	1600	60->52	0	50	250	425	Baseline
2	12	65.5	7/27/95 1:30	7/27/95 13:30	#7	70	1025	1600	52	0	50	225	425	Underflow Nitrogen
3	12	77.5	7/27/95 13:30	7/28/95 1:30	#7	70	1025	1600	52	0	50	280	425	
4	12.75	90.25	7/28/95 1:30	7/28/95 14:17	#7	70	1025	1600	52	0	50	250	425	
5	11.3	101.55	7/28/95 14:17	7/29/95 1:30	#7	70	1025	1600	47	0	50	250	425	Reactor Steam
6	12.43	113.98	7/29/95 1:30	7/29/95 13:50	#7	70	1025	1600	52	0	50	250	425	
7	2.5	116.48	7/29/95 13:50	7/29/95 16:20										Hot-Hold
	3.75	120.23	7/29/95 16:20	7/29/95 20:00	Fired rupture disc on secondary cyclone									Fill Bed
	5.5	125.73	7/29/95 20:00	7/30/95 1:30	#7	70	825->1025	1600	52	0	50	250	425	Stabilization
	13.25	138.98	7/30/95 1:30	7/30/95 14:42	#7	70	1025	1600	52	0	50	250	425	Cone
8	10.75	149.73	7/30/95 14:42	7/31/95 1:30	#7	70	1025	1600	57	0	50	250	425	Steam
9	12	161.73	7/31/95 1:30	7/31/95 13:30	#7	70	1025->1400	1600	57	0	50	250	425	Coal Feed Rate
10	12	173.73	7/31/95 13:30	8/1/95 1:30	#7	80	1400	1600	57	0	50	250	425	Baseline
11	9	182.73	8/1/95 1:30	8/1/95 10:30	#7	70	1025	1600	52	0	50	250	425	Reactor Air
12	75.42	258.15	8/1/95 10:30	8/4/95 13:49	#7	70	1085	1600	52	0	50	250	425	Hot-Hold
	11	269.15	8/4/95 13:49	8/5/95 0:47	Allowing MGCR to load the sorbent									Baseline
13	4.3	273.45	8/5/95 0:47	8/5/95 5:10	#7	70		1600	52	0	50	250	425	Shut Down
	14.3	287.75	8/5/95 5:10	8/5/95 20:00	Loss of coal feed due to clinker									Heat Up
	3.85	291.6	8/5/95 20:00	8/5/95 23:50		0	4000	0	0	0	0	250	425	Combustion/ Fill Bed
	1.75	293.35	8/5/95 23:50	8/6/95 1:35	#7	12	4000	800	0	0	0	250	425	Stabilization
	4	297.35	8/6/95 1:35	8/6/95 5:30	#7	12->70	500->1085	1600	52	0	0	250	425	Sorbent Test
14	16.5	313.85	8/6/95 5:30	8/6/95 22:00	#7	70	1085	1600	52	0	0	250	425	Coke Breeze
15	12	325.35	8/6/95 22:00	8/7/95 10:00	Coke Breeze	70	1085	1600	55	0	0	400	425	Shut Down
	8.83	334.58	8/7/95 10:00	8/7/95 18:50	Lost of Rx Air and Steam due to Clinker									Combustion/ Fill Bed
	1.44	336.12	8/7/95 18:50	8/7/95 20:15	Coke Breeze	70	500->1085	1600	0	0	0	400	425	Stabilization
16	5.4	341.52	8/7/95 20:15	8/8/95 1:35	Coke Breeze	70	1085	1600	55	0	0	400	425	
17	0.1	341.62	8/8/95 1:35	8/8/95 1:40	Blackville Coal	70	1085	1600	55	0	0	400	425	Bituminous Coal
	18.38	360	8/8/95 1:40	8/8/95 20:00	Cool Down									Cool Down/ Shut Down

* Old Baseline (94FBG10). ** New Baseline (95FBG12) *** Total Gasification Time = 261 hours % availability = 82% (319 hrs = 100%)

Table 3: Test Matrix Completed for 95FBG11 (July 24 - Aug 8, 1995)

	Outlet Flow	Upper Bed Temps	Lower Bed Temps	PDIR718	Reactor P PIC 713
Reactor Air	$\frac{3.33}{32s+1}$	$\frac{0.52}{30s+1}$	$\frac{0.85}{30s+1}$	$\frac{0.083}{5s+1}$	$\frac{0.083e^{-60s}}{50s+1}$
Reactor Stm		$\frac{-2,3}{42s+1}$	$\frac{-3.6e^{-33s}}{50s+1}$		
Underfl N2				$\frac{.055}{44s+1}$	$\frac{.052}{42s+1}$
Cone Steam		$\frac{-2.3}{46s+1}$		$\frac{.833}{12s+1}$	
Coal Feed		$\frac{2.6e^{-62s}}{48s+1}$	$\frac{-10e^{-55s}}{58s+1}$		

Table 4A: Partial transfer function matrix derived from gasifier run 11.
Empty elements indicate no detectable change in output,

	CH4 Comp	C02 Comp	CO Corn	N2 Comp	
Reactor Air	$\frac{-0.003}{32s+1}$	$\frac{-0.0167}{34s+1}$	$\frac{-0.035}{31s+1}$	$\frac{0.0167}{32s+1}$	
Reactor Stm					
Underfl N2					
Cone Steam					
Coal Feed		no data	no data		

Table 4B: Partial transfer function matrix derived from gasifier run 11,
Empty elements indicate no detectable change in output.

111. Fluid Bed Gasifier Control

With the exception of some simple flow controllers on inlet steam and air flows, present successful operation of the FBG is dependent upon the expertise of process operators. Part of their strategy for controlling the FBG under steady operation is to use inlet air flow to control the maximum bed temperature and steam flow to control the moisture content of the exit gas. Coal feed is used to control hopper level. During transient periods such as startup or switch to gasification mode, the operation is more

complex, however, we will focus on improving gasifier operation under steady conditions in this study. To do this, we will examine two critical issues, first improving performance of backpressure and MGCR controllers, and second, examining the interaction between steam and air flows and proposing a multivariable controller to eliminate process interactions between them.

Backpressure and MGCR control play an important role in the ability of the operator to run the gasifier successfully. In gasifier run #12, the backpressure controller caused cycling in reactor pressure and was a cause of major operational problems.

IV. Backpressure and MGCR Control

Good pressure control is critical to successful operation of the FBG. Fluctuations in gasifier pressure affect inlet gas flowrates, gasifier temperatures, and downstream MGCR pressure. Over the last several gasifier runs, the FBG backpressure has been controlled using a split-range automatic controller, Most of the time this controller maintains the pressure within plus or minus 5 psi of setpoint. However, frequently the controller overreacts and the pressure swings dramatically. If the operator does not take the proper intervention steps immediately, the pressure swings will shut down the gasifier. This section identifies several sources of problems with the present pressure control system and then suggests modifications to the present scheme.

i. Problems with the present control scheme

Below are summarized some of the major problems with the present backpressure controller.

1. *Split-range control scheme:* A large valve and a small valve operating in parallel are manipulated in order maintain desired FBG pressure. The small valve opens first to control pressure at low to moderate make-gas flowrates, while the large valve remains closed. At high make-gas flows, the small valve is open completely, and the large valve is manipulated to maintain pressure. At the operating condition used in the first four days of 95FBG 11, the make-gas flow was such that the split-range controller operated at the crossover point from the large valve to the small valve (that is, the large valve closed, the small valve open). One can not expect good control in this regi on.

2. *Interactions with the MGCR pressure controller:* The MGCR pressure fluctuates due to a large dead time between the upstream valve and the vessel pressure (V-100). Fluctuations in the valve controlling the MGCR pressure (PV-254) affect the backpressure controller.

3. *Upstream disturbances:* The inlet gas flow controllers interact with the backpressure. Changes in inlet gas flowrates will affect gasifier pressure. Similarly gasifier pressure will affect inlet flow of gases. Most of the time when the gasifier backpressure cycles, so do the inlet gas flows.

4. *Controller tuning:* Optimal controller tuning parameters will change as the operating condition changes, For example, one would expect markedly different tuning parameters in the backpressure controller under conditions where the large valve is adjusted than under conditions where the small valve is being adjusted. In one observed instance, the backpressure loop was swinging rather dramatically. The operator on duty intervened by simply putting the controller in manual and maintaining a constant valve position. Almost immediately, the backpressure stabilized. This points to poor controller tuning.

5. *Buildup of solids at the control valve:* There is evidence to suggest that fine solids particles are accumulating just upstream of the control valve. In one case, backpressure was oscillating continuously with increasing amplitude. Finally, the pressure swings were large enough to force solids out of the gasifier and into the incinerator (and damaging the incinerator). After this 'burp' gasifier control was very good for a long period of time.

ii. Suggested modifications to **backpressure** and MGCR pressure controllers,

The following modifications are suggested in order to eliminate backpressure control problems:

A. Backpressure controller

1. Replace the split-range configuration with the following: Two valves placed in parallel (similar to the present configuration). One valve should be tied to a PID

controller and will directly control FBG backpressure. This valve should be sized to cover the range of desired operating conditions. A second, larger valve will be used to letdown system pressure quickly. This valve can only be manipulated manually or through a safety override. With this configuration, under normal, steady operation of the gasifier, the large valve will remain static and the controller will manipulate the other valve to maintain backpressure.

2. Install a purge system to remove solids accumulation in the exit line.

3. Establish good controller tuning guidelines - how controllers should be tuned and who should tune them. An autotuning facility available in most DCS's should be most useful.

B. MGCR pressure control

1. Implement a cascade control arrangement to reduce the large time lag between valve V-254 and vessel V-100, In a cascade arrangement, an inner controller would control the pressure just downstream of the valve V-254 or in the particulate removal vessel, F-100. The outer or master controller maintains the pressure in V-1OO by adjusting the setpoint of the inner controller. The result is a control system that responds much faster and rejects disturbances in upstream pressure.

C. Diagram of suggested backpressure and MGCR pressure control scheme.

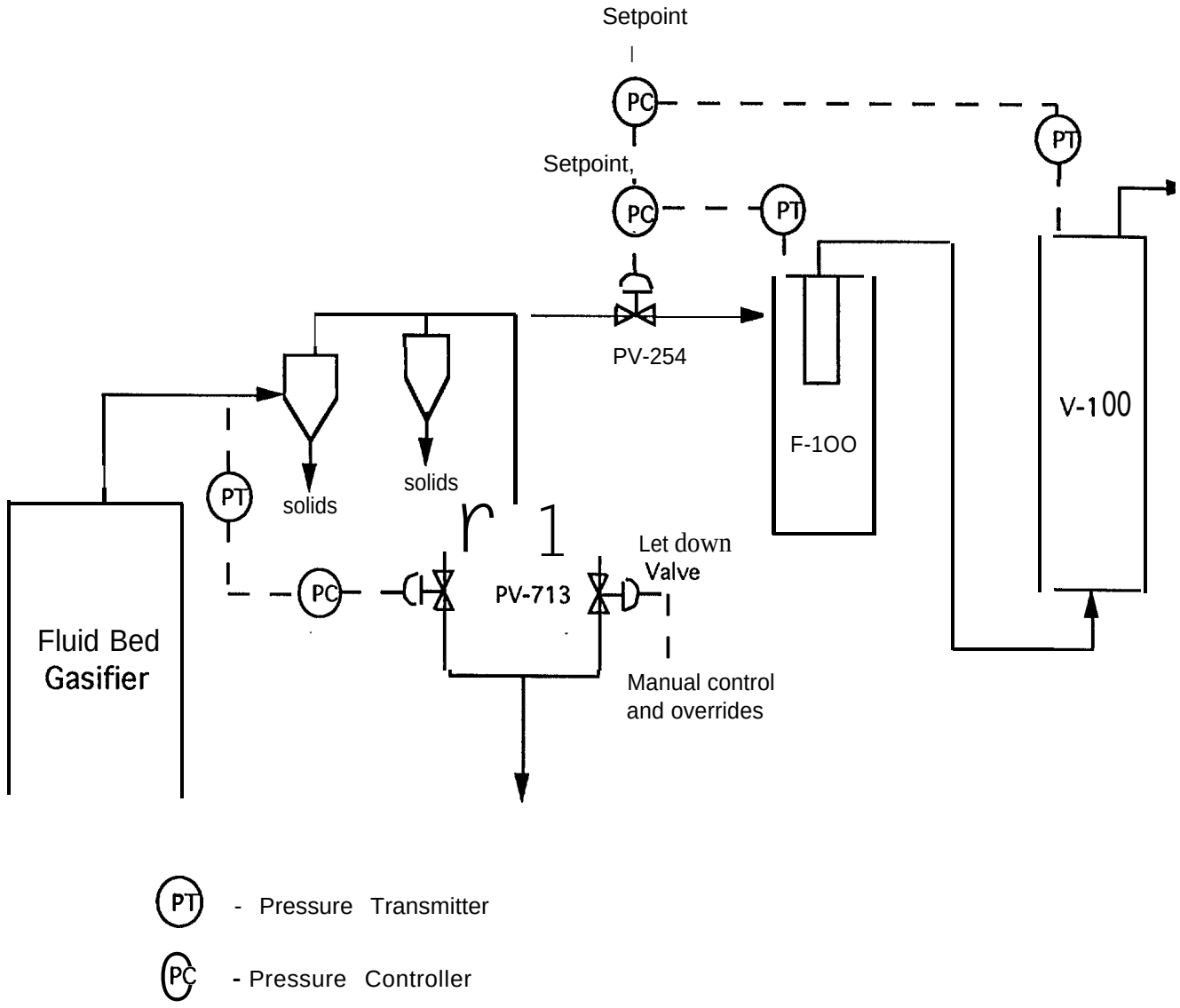

Figure 1- Suggested FBG backpressure and MGCR pressure control scheme

V. Control of Bed Temperature and Moisture Content

Improvement of the backpressure controller will greatly improve ease of FBG operation, however, it will not eliminate interactions between process inputs. It is clear that process operators have a complex decision making process during transient operation of the gasifier. Design of a multivariable control scheme which takes into account all of the operational constraints during all modes of operation is well beyond the scope of what can be accomplished from the limited number of successful test runs that have been made, However, we will present a simple analysis of the control of maximum bed temperature and exit gas moisture content (using inlet air and steam flow) during steady operation. We will then outline a 2-input, 2-output model based controller which can be implemented to minimize interactions and improve performance. The model based controller will be useful for both setpoint tracking and disturbance rejection.

i. Interactions

During steady operation of the FBG, operators typically control the maximum bed temperature using air flow and control exit gas moisture content using inlet steam flow. The gain matrix for this simple 2-input, 2-output sub-system can be constructed from the transfer function matrix given in Section II (moisture content numbers were calculated from MGAS simulations).

$$\overline{K} = \begin{array}{c} \\ F_{air} \\ F_{st} \end{array} \begin{array}{c} \begin{array}{cc} T_{bed} & Y_{H_2O} \end{array} \\ \begin{bmatrix} 0.51 & -0.167 \\ -2.01 & 0.110 \end{bmatrix} \end{array}$$

The resulting Relative Gain Array is

$$\Lambda = \begin{array}{c} \\ F_{air} \\ F_{st} \end{array} \begin{array}{c} \begin{array}{cc} T_{bed} & Y_{H_2O} \end{array} \\ \begin{bmatrix} 2.55 & -1.55 \\ -1.55 & 2.55 \end{bmatrix} \end{array}$$

The RGA indicates that for single-input, single-output control, air flow should control bed temperature and steam flow should control moisture content (consistent with present manual control). Note that pairing air with moisture content and steam with temperature

would lead to a potentially unstable control scheme. The RGA also reveals a significant degree of process interaction (a value of 2.55 is quite large for a 2x2 system). Significant improvement in control can potentially be achieved by using a multivariable controller.

ii. Dynamic Matrix Control

The last 15 to 20 years have seen the development of several control concepts based on using a model of the process within the controller. Perhaps the most successful of these model based controllers is Dynamic Matrix Control (DMC). DMC was developed at Shell Oil Company in 1979 by C.R. Cutler and B. L. Ramaker. Its basic concept is to use a time-domain step response model of the process to calculate future manipulated variable moves which minimize a performance index. This report will discuss the basics of DMC and then illustrate the method through an example implementation on the gasifier. A more detailed discussion is given in several references [Luyben, W.L. Process Modeling, Simulation, and control for Chemical Engineers, McGraw Hill, and Cutler, C.R. and Ramaker, B. L., "Dynamic Matrix Control -- A Computer Control Algorithm," 86th Meeting of AIChE].

DMC Model

The DMC modeling approach must first be explained before the control algorithm can be presented. The discussion will focus on a single-input, single-output system for simplicity, but we will also show that the extension for the mult-input, multi-output case is straightforward.

As mentioned above, the model is based on the step response of the process, As illustrated below a step change in the manipulated variable is made (AU). The output at each sampling time, kT, is recorded until the process has reached a new steady-state. As illustrated in Figure 2 below, dynamic coefficients, ai, are defined at each sampling time,

$$a_i = X_i/AU.$$

where Xi is the change at each time sample in output relative to the initial condition.

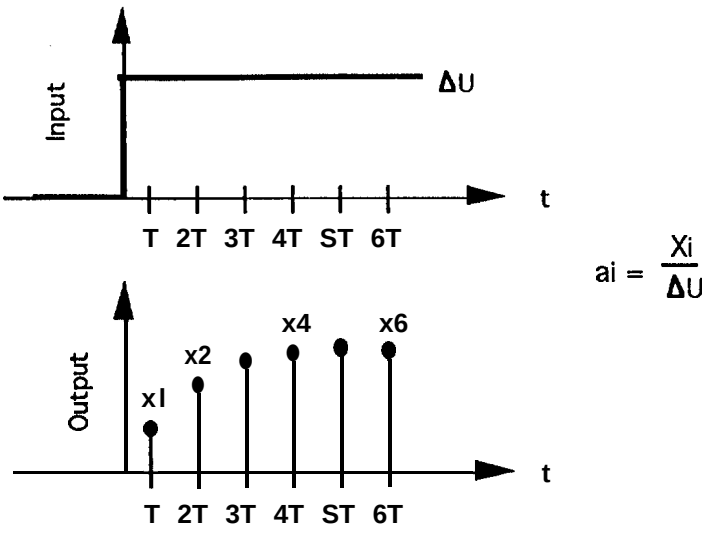

Figure 2: Discrete response of process output to step change ininput

For N future time samples

$X_1 = a_1 \Delta U$
X2= a2AU
X3= a3AU or $\underline{X} = \underline{A}\Delta U$

X_N = aNAU.

Assuming that thesystem is linear, theoutput can bepredicted inthismanner for any single input. For a series of inputs implemented at successive time steps (as shown in Figure 3 below),

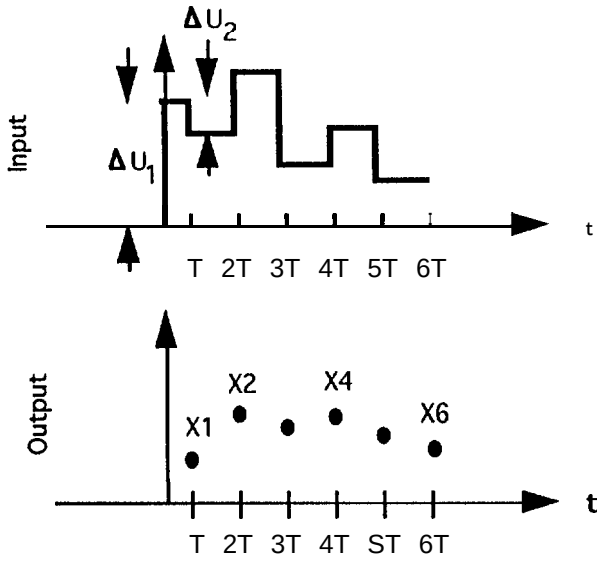

Figure 3: Process output resulting from a series of input changes

the output can be predicted by

$$X_1 = a_1\Delta U_1$$
$$X_2 = a_2\Delta U_1 + a_1\Delta U_2$$
$$X3 = a_3\Delta U_1 + a_2\Delta U_2 + a_1\Delta U_1$$
$$\cdot$$
$$X_N = a_N\Delta U_1 + a_{N-1}\Delta U_2 + a_1\Delta U_N$$

which can be written in matrix notation as

$$\underline{X} = \underline{A}\underline{\Delta U}$$

or

$$\begin{vmatrix} X_1 \\ X_2 \\ X_3 \\ X_4 \\ \\ X_N \end{vmatrix} = \begin{vmatrix} a_1 & O & 0 & . & . & 0 \\ a_2 & a_1 & O & 0 & . & 0 \\ a_3 & a_2 & a_1 & O & . & 0 \\ a_4 & a_3 & a_2 & . & . & o \\ & & & . & . & . \\ a_N & a_{N-1} & \%.2 & " & " & a_1 \end{vmatrix} \begin{vmatrix} \Delta U_1 \\ \Delta U_2 \\ \Delta U_3 \\ \\ \\ \Delta U_N \end{vmatrix}$$

In this case **A** is NxN (N outputs predicted from N inputs). It is often desirable in DMC to predict M outputs from N inputs. In that case **A** becomes MxN.

For the multi-input, multi-output case, the model is analogous to a transfer function matrix, **G(s)**.

$$\overline{G}(s) = \begin{bmatrix} G_{11}(s) & G_{12}(s) & . & . & G_{1q}(s) \\ G_{21}(s) & G_{22}(s) & , & . & G_{2q}(s) \\ & & . & . & . \\ . & & & . & . \\ G_{p1}(s) & G_{p2}(s) & . & . & G_{pq}(s) \end{bmatrix}$$

where Gij (s) represents the relationship of the ith output to the jth input. An analogous model is formed for DMC, with **Aij** representing the relationship between the ith output and the jth input. The overall system dynamic matrix, **A**, is then a matrix of smaller matrices

$$\overline{A} = \begin{bmatrix} \overline{A}_{11} & \overline{A}_{12} & . & . & \overline{A}_{1q} \\ \overline{A}_{21} & \overline{A}_{22} & . & . & \overline{A}_{2q} \\ . & . & . & . & . \\ . & . & . & . & . \\ \overline{A}_{p1} & \overline{A}_{p2} & . & . & \overline{A}_{pq} \end{bmatrix}$$

The process is then modeled by **X** =&J

where

$$x = \begin{bmatrix} X_1 \\ X_2 \\ \\ \\ p^x \end{bmatrix} = \text{process output vector}$$

$$u = \begin{bmatrix} U_1 \\ U_2 \\ . \\ . \\ U_q \end{bmatrix} = \text{input vector.}$$

The discussion will now return to single-input, single-output. The prediction of the process output by the DMC model discussed so far requires the knowledge of future process inputs. This model is useful for studying the anticipated result of a series of future control moves, but is of little use if the future control moves are not yet known. A prediction vector, $\underline{P}$ (dimension Nx1), is defined which contains the prediction of the process outputs based on process inputs up to the present time, assuming that the process input remains constant in the future. The prediction vector can be updated recursively at each time step by

$$P_{i,new} = P_{i+1,old} + a_{i+1}\Delta U$$

where

AU= change in process input from previous time sample

$i = 1, N-1$

The prediction vector is usually initialized equal to the process output at the time DMC is implemented.

DMC Algorithm

This section will discuss the control algorithm of DMC. In Figure 4 below, the process has been operation for some time so that the process output is predicted from the prediction vector N time steps into the future,

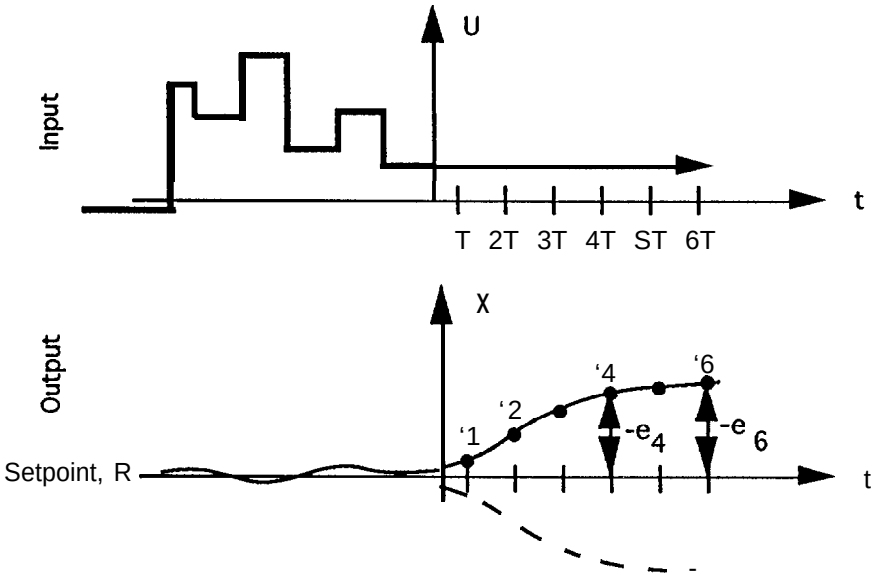

Figure 4: Illustration of prediction vector, P

The goal of the DMC algorithm is to find a future set of inputs which will minimize error from setpoint over a future time horizon,

$$\underline{E} = [e_1, e_2, \ldots . eN]^T = \text{error vector}$$

where

$$ei = R - Pi.$$

R = Setpoint

If one could find a set of future inputs to give a response represented by the dotted line, then, when added together, the effects of past inputs and future inputs will give Xi = R, Such a set of future inputs, AUi is what the DMC algorithm seeks.

It is now necessary to find the equation for the dotted line in terms of inputs AUi. Recall the DMC modeling equation, $\underline{X} = \underline{\mathbf{A}}\Delta\underline{U}$, where $\underline{X}$ is the output due to the set of inputs, $\Delta\underline{U}$. It can be seen from Figure 4 that the dotted line is given by the equation

$$\underline{E} = \underline{\mathbf{A}}\Delta\underline{U}.$$

The error vector, $\underline{E}$, is known at each time step from the prediction vector, and the dynamic matrix, $\mathbf{A}$, is a constant matrix formed from step test modeling. The desired set of future inputs can then be found simply by

$$\Delta\underline{U} = \mathbf{A}^{-1}\underline{E}$$

However, the dynamic matrix, $\mathbf{A}$ is often poorly conditioned (near singular) and the above equation results in erratic manipulated variable movement. Instead the pseudo inverse of $\mathbf{A}$ is calculated by one of the two methods given below.

1. $\mathbf{A}^{+} = \underline{V}\Sigma^{-1}\underline{U}^{T}$
   where
   I-J, Σ, and $\underline{V}$ are calculated from the Singular Value Decomposition (SVD) of $\mathbf{A}$

2. $\mathbf{A}^{+} = [\mathbf{A}^{T}\mathbf{A} + f^{2}\underline{I}]^{-1}\underline{\mathbf{A}}^{T}$
   where f is an input move suppression factor.

Using the pseudo inverse, the control moves are calculated by the equation

$$\Delta\underline{U} = \mathbf{A}^{+}\underline{E}.$$

Summary of DMC

The following basic steps comprise the DMC algorithm:

1, Step tests to obtain the dynamic matrix, $\underline{\mathbf{A}}$.
2, Initialize prediction vector, $\underline{P}$.
3. Given $\underline{P}_{old}$, calculate $\underline{P}_{new}$.
4. Calculate $\underline{E}$ by $e_i = R - Pi$.
5. Calculate next N control moves by $\underline{\Delta U} = \underline{\mathbf{A}}^T \underline{E}$.
6. Implement the first calculated control move.
7. Go to step 3 for next time step,

Notes

1. At each time step, a prediction vector is calculated and an actual process output is measured. A feedback bias can be calculated by

$$f = X - P_{1,old}$$

where X = measured output

The new prediction vector can then be adjusted by

$$Pi' = Pi + f.$$

2. The number of future inputs calculated and the number of prediction vector elements are DMC tuning parameters.

3. $\underline{\mathbf{A}}^+$ can be calculated off-line and stored in memory so that no matrix inversion is required at each time step. There are methods of adjusting $\underline{\mathbf{A}}^+$ on-line so that the algorithm becomes adaptive for nonlinear or time varying systems.

4. The method is independent of the complexity of dynamics (dead-time, inverse response, etc).

5. By using the pseudo-inverse, the following index is minimized:

$$\| \mathbf{A}\overline{U} - \overline{E} \|_2^2$$

6. The DMC algorithm outlined above does not include constraint handling. For example suppose it is desired that $AU_{min} < AU < AU_{max}$.

The problem then becomes

minimize $\|\mathbf{A}\overline{U} - \overline{E}\|_2^2$

subject to $C\Delta U > b$

This problem can be solved using Quadratic Programming (QP). The method then becomes the Quadratic Programming solution to DMC (QDMC) [Garcia, C.E. and Morshedi, A. M., "Quadratic Programming Solution of Dynamic Matrix Control (QDMC)," Chemical Engineering Communications, 1986].

iii. Example implementation

The following example is meant to illustrate an implementation of the basic DMC algorithm on a 2-input, 2-output system related to the FBG. The inputs will be reactor air and steam, and the outputs are maximum bed temperature and exit moisture content. We will assume the following process relationship for simplicity.

$$\begin{bmatrix} T_{max} \\ Y_{H2O} \end{bmatrix} = \begin{bmatrix} \frac{0.5}{30s+1} & \frac{-2.0}{42s+1} \\ \frac{-0.0167}{95s+1} & \frac{0,110}{95s+1} \end{bmatrix} \begin{bmatrix} F_{air} \\ F_{steam} \end{bmatrix} 1$$

Clearly this model is limited in its accuracy in predicting numbers from the FBG behavior, and the numbers calculated in this example should not be applied directly on the FBG. However, the example does serve as a reasonable process for illustrating DMC.

Formation of the dynamic matrix

Responses of the two process outputs to step changes in both process inputs are shown in Figure 5. The resulting dynamic coefficients for each response are shown in the Figure. Note that in order to illustrate the method (i.e., to minimize the size of&, only five dynamic coefficients for each response will be used. Typically more coefficients should be used so that the entire response is represented in the dynamic matrix. These dynamic vectors are given by:

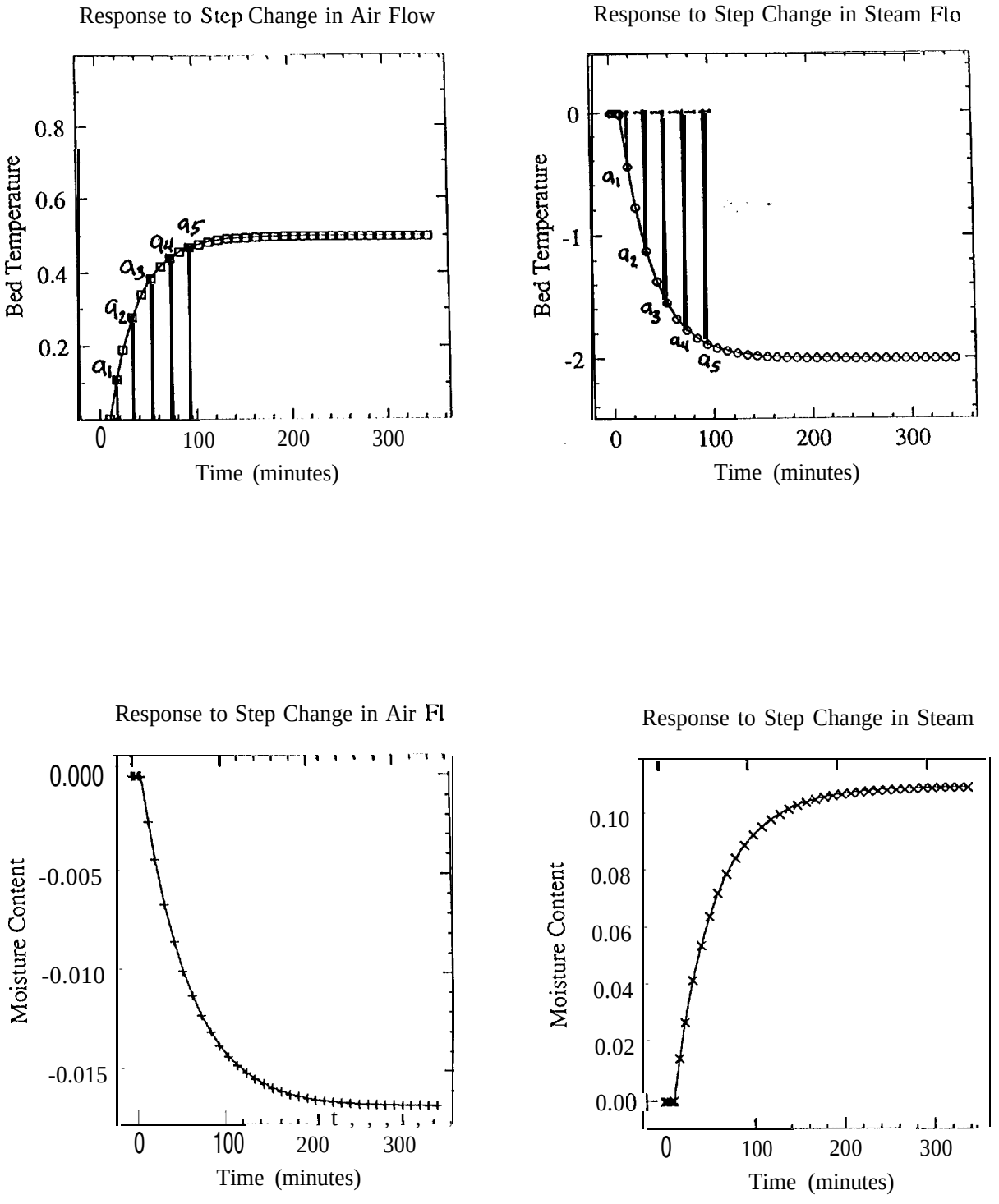

Figure 5: Open Loop Responses to Step Changes in A) air flow and B) steam flow

A_{11}^T = [.0035, .279,.419,.470, .489]

A_{12}^T = [-.0392, -1.118, -1.675, -1.881, - 1.956]

A_{21}^T = [$-6{,}98 \times 10^{-5}$, -6.48×10^{-3}, -1.11×10^{-2}, -1.36×10^{-2}, -1.50×10^{-2}]

A_{22}^T = [4.60×10^{-4}, 4.27×10^{-2}, 7.31×10^{-2}, 8.97×10^{-2}, 9.89×10^{-2}]

These vectors may need to be scaled depending upon the control system. A controller which inputs and outputs its information in terms of percent of span would require scaling of the dynamic vectors. We will assume this is the case and scale the vectors. The scaling factors for each are given by:

$$\text{scaling factor} = \frac{\frac{1}{\text{span of output}}}{\frac{1}{\text{span of input}}}$$

In this example, the following ranges were used:

inputs: span of air flow :1025 (baseline value for air flow)
span of steam flow: 57 (baseline value for steam flow)
outputs: span of max bed temp: 1000 (500 -1500 deg F)
span of moisture content: 100 (O -100 percent)

The resulting scaled vectors are:

A_{11}^T = [.00238, .199, .285,.320, .333]

A_{12}^T = [-.0015, -.0425,-.0637,-.071, -,074]

A_{21}^T = [-.00072, -.0663, -.1 14,-.140,-.154]

A_{22}^T = [.00026, .0243,.0416, .0511, .0564]

The resulting dynamic vector, $\underline{A}$ is

$$\underline{A} = \begin{bmatrix}
.0024 & 0 & 0 & 0 & 0 & -.00150 & 0 & 0 & 0 \\
.199 & .0024 & 0 & 0 & 0 & -.0425 & -.00150 & 0 & 0 \\
.285 & .199 & .0024 & 0 & 0 & -.0637 & -.0425 & -.00150 & 0 \\
.320 & .285 & .199 & .0024 & 0 & -.071 & -.0637 & -.0425 & -.00150 \\
.333 & .320 & .285 & .199 & .0024 & -.074 & -.071 & -.0637 & -.0425 \\
-.00070 & 0 & 0 & 0 & . & 0 & 0 & 0 & 3 \\
-.0633 & -.00070 & 0 & 0 & .0243 & .0003 & 0 & 0 & 0 \\
-.114 & -.0633 & -.00070 & 0 & .0416 & .0243 & .0003 & 0 & 0 \\
-.140 & -.114 & -.0633 & -.00070 & .0511 & .0416 & .0243 & .0003 & 0 \\
-.154 & -.140 & -.114 & -.0633 & -.0007 & .0564 & .0511 & .0416 & .0243
\end{bmatrix}$$

Formation of the pseudo-inverse

The pseudo-inverse, $\underline{A}^+$ was calculated by $\underline{A}^+ = [\underline{A}^T\underline{A} + f^2\underline{I}]^{-1}\underline{A}^T$ where f = 0.5. The result is given below.

$$A^+ = \begin{bmatrix}
0.0030 & 0.262 & 0.282 & 0.238 & 0.197 & -0.0009 & -0.0816 & -o.117 & -o.110 & -0.095 \\
-0.0012 & -0.0889 & 0.177 & 0.240 & 0.241 & 0.0003 & 0.0295 & -0.0428 & -0.0904 & -0.102 \\
-0.0007 & -0.0519 & -0.125 & 0.180 & 0.288 & 0.0002 & 0.0171 & 0.0476 & -0.0378 & -0.105 \\
-0.0003 & -0.0195 & -0.0509 & -0.0864 & ‘0.266 & 0.0001 & 0.0064 & 0.0191 & 0.0352 & -0.070 \\
-0.0000 & -0.0002 & -0,0006 & -0.0011 & 0.0032 & 0,0000 & 0.0001 & 0.0002 & 0.0004 & -0.00(\\
-0.0026 & -0.0517 & -0.0572 & -0.0438 & -0.0338 & 0.0005 & 0.0376 & 0.0560 & 0.0605 & 0.060 \\
0.0003 & 0.0200 & -0.0313 & -0.0471 & -0.0453 & -0.0001 & -0.0070 & 0.0281 & 0.0496 & 0.058 \\
0.0002 & 0.0127 & 0.0287 & -0.0322 & -0.0594 & -0.0000 & -0.0042 & -0.0114 & 0.0270 & 0.053 \\
0.0001 & 0.0047 & 0.0123 & 0.0188 & -0.0538 & -0.0000 & -0.0016 & -0.0046 & -0.0082 & 0.035 \\
0.0000 & 0.0001 & 0.0004 & 0.0006 & -0.0021 & -0.0000 & -0.0000 & -0.0001 & -0.0003 & 0.000
\end{bmatrix}$$

Manipulated variable calculation

A horizon of future control moves are calculated at each time step by $\underline{\Delta U} = \underline{A}^+\underline{E}$. Only the first input change is actually implemented and a new input horizon is calculated at the next time step. As an example, assume that the process has been at setpoint for some time and at the present time sample a step change of 3.0 in both max bed

temperature and moisture concentration setpoints are made (ignoring the fact that 3 degrees F is unreasonably small for temperature on the FBG). The resulting error vector will be

$$\bar{E} = [3.0,\ 3,0,\ 3.0,3.0,\ 3.0,3.0,\ 3.0,3.0,\ 3_{\$}0,\ 3.0]^T$$

and the resulting input horizon is

$$\Delta\bar{U} = [.395,\ .423,\ .247,\ ,112,.0015,.0424,\ .0128,\ .00612,\ -.000231,\ -.00124]$$

(calculated from $\Delta\underline{U} = \underline{A}^{+}\underline{E}$).

Improvement in response

Figure 6 shows the response of the system for the setpoint changes described above when S1S0 PID control is implemented on the system. Due to control loop interactions, each loop must be detuned to avoid rapid movement of control valves. As a result, the responses are quite sluggish. Figure 7 illustrates the same setpoint changes made on a completely decoupled system using the DMC algorithm. One can see a dramatic improvement in shape and speed of response.

An important note

A comparison of Figure 6 with 7 illustrates the potential improvement attainable with DMC. A multivariable, model-based controller like DMC will automatically compensate for interactions between control loops, and thus there is potential for significant improvement. However, one should be aware that the success of DMC hinges upon the ability to obtain a good step response model in the area of a given operating point. Any model-based controller implemented using an inaccurate model will generally perform worse than classical S1S0 PID type control.

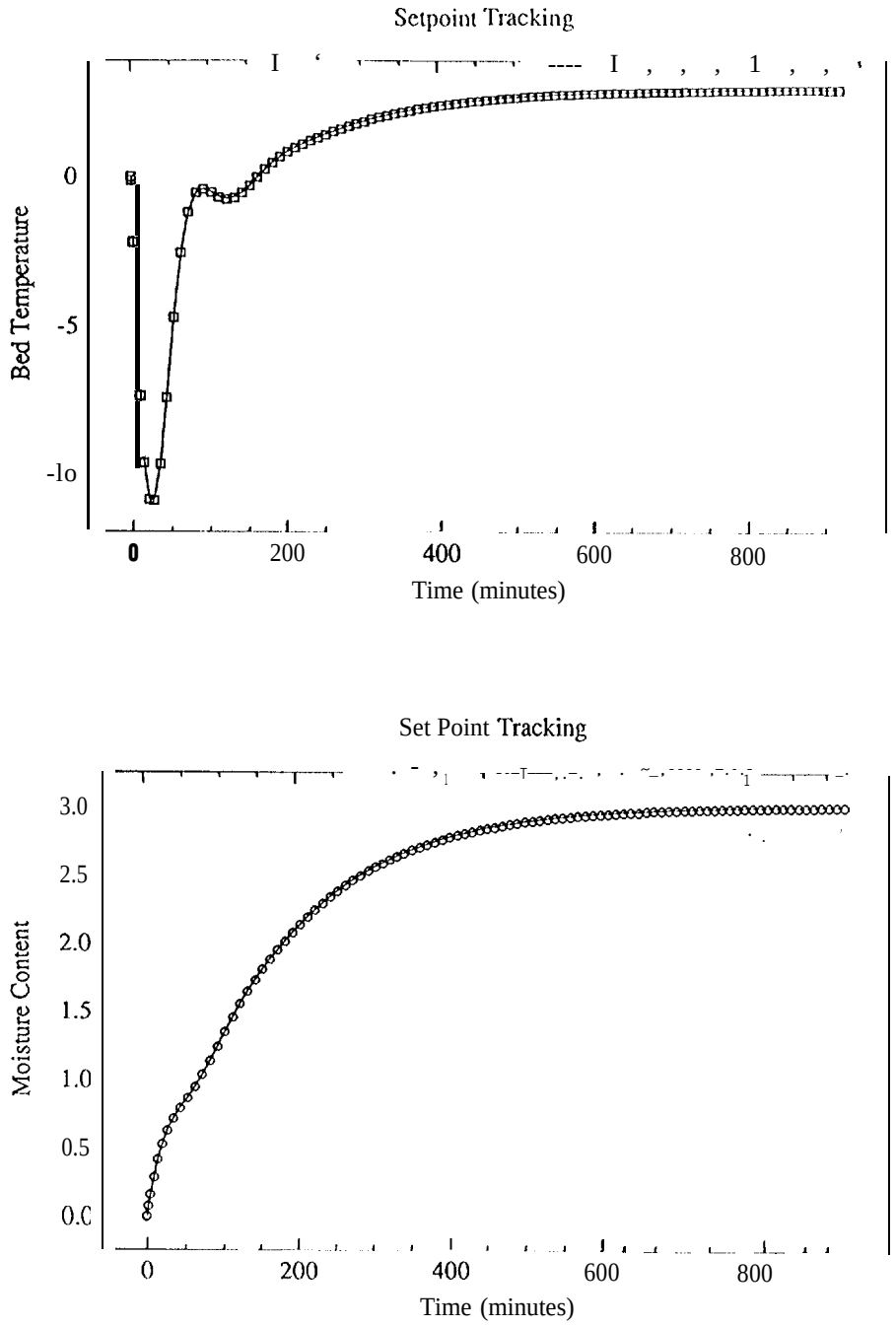

Figure 6: Responses of bed temperature and moisture content under single-input, single-output PID control when simultaneous step changes in setpoint.

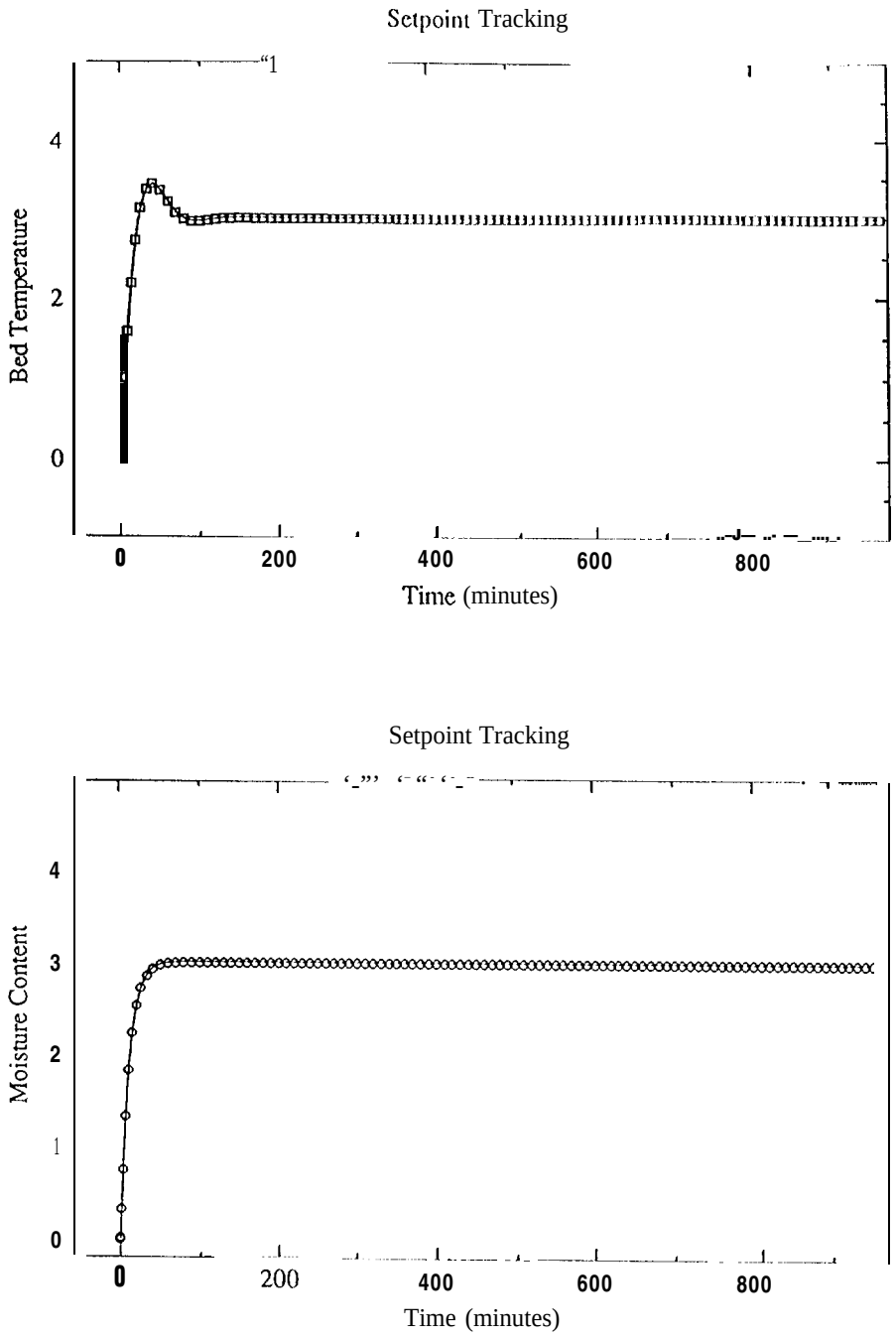

Figure 7: Responses of bed temperature and moisture content under DMC to simultaneous step changes in setpoint.

VI. **Conclusions**

Present operation of the FBG is the result of experience and expertise gained over man y years, It is important that any implementation of automatic control be implemented by taking small, managable steps, and keeping the operators involved during each step of the process. This study has presented two small control system modifications which should contribute to the ease of FBG operation and help to prevent unplanned shutdowns. Improvement in the FBG and MGCR pressure control loops will improve performance of all flow control loops and enhance the ability to analyze gasifier data from open loop step tests. Implementation of a multivariable model-based controller on the inlet steam and air flows will decouple the two control loops resulting in faster overall response times. While the improvement realized in the application of DMC will likely not be as significant as that realized from improving pressure control, the DMC! application represents a simple application of advanced control. Once successful, the DMC algorithm can be applied to the FBG on a much larger scale.

Appendix I

ANALYSIS AND CONTROL OF THE METC FLUID BED GASIFIER

Technical Progress Report for the Period 10/1/94 - 1/31/95

By:
Andrew E. Farell
Sadanand Reddy
Chemical Engineering Department
University of South Carolina
Columbia, SC

Work performed under Contract No.: DE-FG21-94MC3 1384

For:
US Department of Energy
Morgantown Energy Technology Center
Morgantown, West Virginia

Table of Contents

I. Overview of Present Work

This document summarizes work performed for the period 10/1/94 to 2/1/95. The initial phase of the work focuses on developing a simple transfer function model of the Fluidized Bed Gasifier (FBG). This transfer function model will be developed based purely on the gasifier responses to step changes in gasifier inputs (including reactor air, convey air, cone nitrogen, FBG pressure, and coal feedrate). This transfer function model will represent a linear, dynamic model that is valid near the operating point at which the data was taken. In addition, a similar transfer function model will be developed using MGAS in order to assess MGAS for use as a model of the FBG for control systems analysis.

II. Discussion of FBG Data

The data for which the transfer function model is developed is taken from gasifier run #1 O (October 1994) only. During the previous gasifier run (run #9), the gasifier was operated over a fairly wide range of operating conditions in an attempt to seek an optimal set of operating conditions. A 'good' condition was identified during run #9. That condition was used as the baseline operating point for run #10 (see Table 1 below).

Coal Type	Montana #7
Coal Feed rate	70 lb/hr
Reactor Air flow	1000 scfh
Convey Air	1600 scfh
Steam flow rate	55 lb/hr
Cone Nitrogen flow	100 scfh
Nitrogen Underflow	300 scfh
Operating Pressure	425 psi

Table 1: FBG Run #10 Baseline Operating Condition

The objective of run # 10 was to make step changes in the cone nitrogen flow, reactor air flow, reactor pressure, steam flow, coal feed rate, and underflow nitrogen flow around this optimal condition.

Gasifier run #10 went smoothly for step changes made in reactor air and cone nitrogen flow. For each, a positive step change followed by a 2X negative step change, and finally a positive step change (back to the original value) were made. The data is reasonably good for these changes in reactor air and cone nitrogen. However, the next scheduled change was reactor pressure which is maintained by a pressure controller (which manipulates the outlet gas flowrate). When a pressure setpoint change was made, it appears that the pressure controller overreacted by closing the valve on the exit stream. This likely had serious consequences on the bed. As a result, the gasifier run was terminated at that point. We therefore report only the part of the transfer function matrix for which data is available from run #10.

Additional data is available from gasifier runs #8 and #9, however, it is unreasonable to develop a linear model over such a wide range of operating conditions. This additional data will be used@ later modeling efforts (see Section VI). The additional data for the transfer function model will be gathered during a run in May 1995.

III. Discussion of Methods Used

This section will discuss the methodology applied in developing transfer function models from the FBG data. This method is typically used in industry for developing simple control relevant models from process data. It will also be used on simulation data from MGAS to evaluate the applicability of using MGAS for control studies on the FBG.

The method for deriving transfer function models involves two steps: first, pose a reasonable form of the model, and second, evaluate model parameters. Defining a reasonable model form is the more important step. In Figures 1 and 2 below, a number of

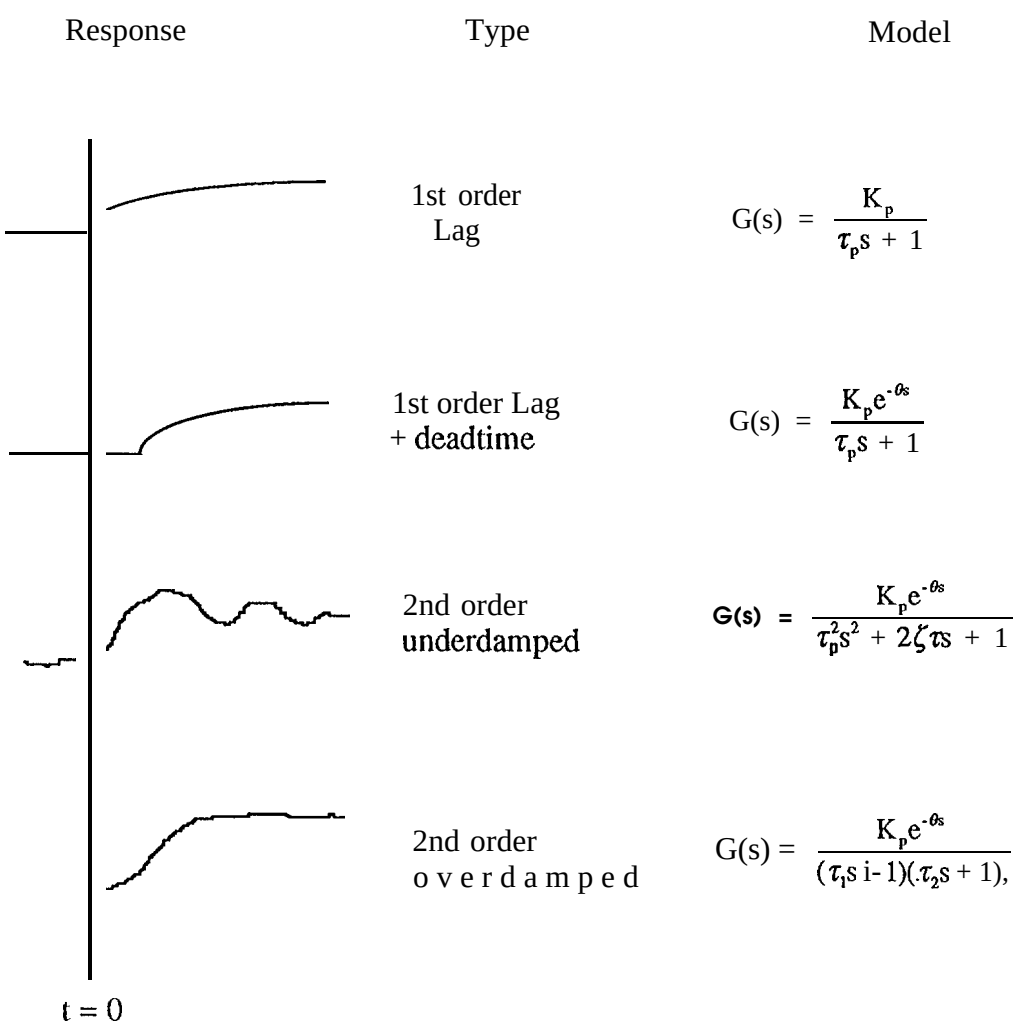

Figure 1: Some common open loop step responses and their appropriate transfer function models

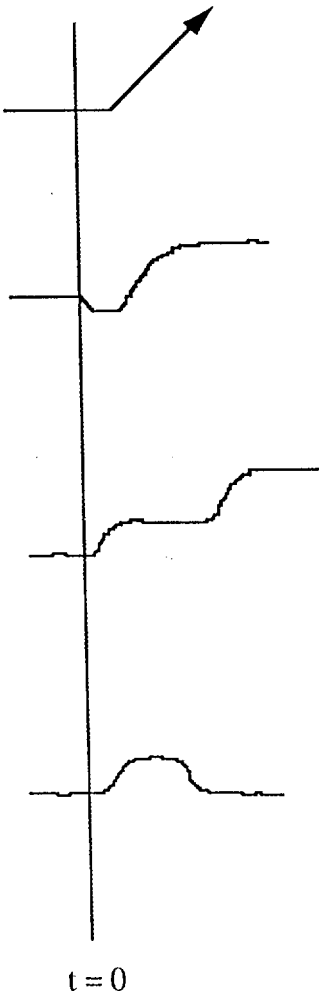

Response	Type	Model
	Pure integrator	$G(s) = \frac{K_p e^{-\theta s}}{s}$
	Inverse response	$G(s) = \frac{-K_1}{\tau_1 s + 1} \frac{K_2 e^{-\theta s}}{\tau_2 s + 1}$ where $K_1 < K_2$
	Stiff process	$G(s) = \frac{K_1}{\tau_1 s + 1} + \frac{K_2 e^{-\theta s}}{\tau_2 s + 1}$ where K_1 and $K_2 > 0$
	Zero gain	$G(s) = \frac{K_1}{\tau_1 s + 1} + \frac{K_2 e^{-\theta s}}{\tau_2 s + 1}$ where K_1 and $K_2 > 0$

Figure 2: Some open loop step responses and their appropriate transfer function models

common 'open loop' step responses are shown along with an appropriate model form for each. 'Open loop' means that there are no automatic control systems on-line.

In Figure 1, the most common model transfer function form used to model plant data is the first order lag plus deadtime (FOLPDT). Complex processes are rarely first order and typically higher order terms are lumped into the deadtime term. For example, a distillation column is comprised of a number of first order systems (column trays) in series resulting in a very high order system. These high order systems are often represented as a FOLPDT. Note that the second order overdamped case can often be modeled reasonably well with a simple FOLPDT. The second order underdamped response is one which can occurs frequently in systems such a RC circuits, along with spring and dashpot systems, but is not all that common in chemical processes. It is theoretically possible for such an open loop response to occur in a reactor system. However, more often than not, such a response is the result of an automatic control system somewhere in the process which is controlling some other process variable.

Figure 2 shows system responses which are more interesting as far as control is concerned. The pure integrator is often seen in tank and accumulator levels in addition to system pressures. Variables which exhibit this type of response can become a problem because they are not self-regulating (they increase without bound). It should also be noted that controlling these variables via automatic control systems can become a problem. If controller gain is set too high or too low, an oscillatory response will result. Since these variables are typically not primary process variables, it is best to control them only within certain bounds rather than controlling them tightly.

The inverse response, stiff process, and zero gain responses are typically the result of competing effects. One effect occurs quickly and the other over a much longer time period. For example, when steam flow is increased to a boiler, the boiler level may actually increase initially due to increased bubbling of the liquid. Over the long run, of course, more liquid will vaporize and the liquid level will drop. The inverse response

represents a particularly difficult control problem. If the controller reacts to the initial output response, it will move the manipulated variable in the wrong direction.

Once an appropriate model for has been identified, model parameters are evaluated. Typically, this is accomplished through standard linear or nonlinear regression. Traditional graphical fitting techniques should be used as a quick check of nonlinear regression results, particularly in cases where higher order systems are approximated with a first order lag plus dead time.

IV. Gasifier Data and Transfer Function Models

Figures 3 through 8 plot 10 second process data, and demonstrate that the responses presented above are seen in the operation of the gasifier. It should be noted that these plots are given for illustration only. A number of phenomenological and operational effects must be factored in to their interpretation. Such a discussion is beyond the scope of this progress report.

V. Transfer Function Matrix from Process Data and from MGAS

Tables 2 through 7 present the transfer function matrix derived from FBG process data during run #10 and from MGAS. As previously discussed, this represents only part of the desired transfer function matrix.

A comparison of the Transfer Function models derived using MGAS with those from the FBG data shows that MGAS gives reasonable results in some cases. In many areas, however, it does not. This is especially true in predicting process time constants. As it has been run in these studies so far, MGAS is inadequate for control studies on the FBG. However, further studies will reconfigure MGAS to include a recirculation of solids from top to the bottom and some adjustment of model parameters.

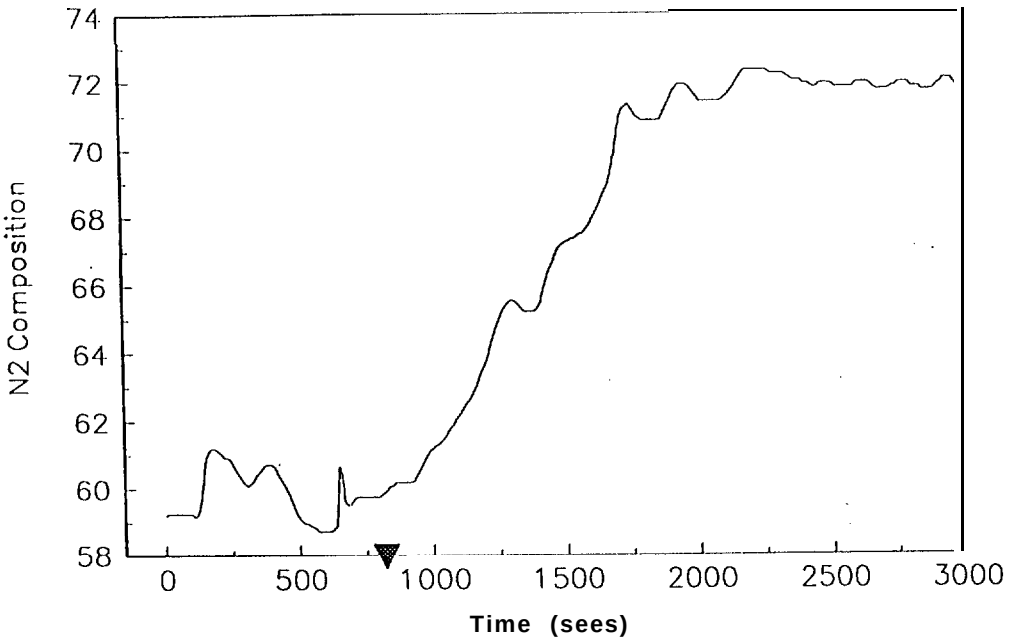

Fig. 3: First Order Response of N2 composition for a change in Cone N2 from 50 to 100 scfh (made at time indicated by ▼).

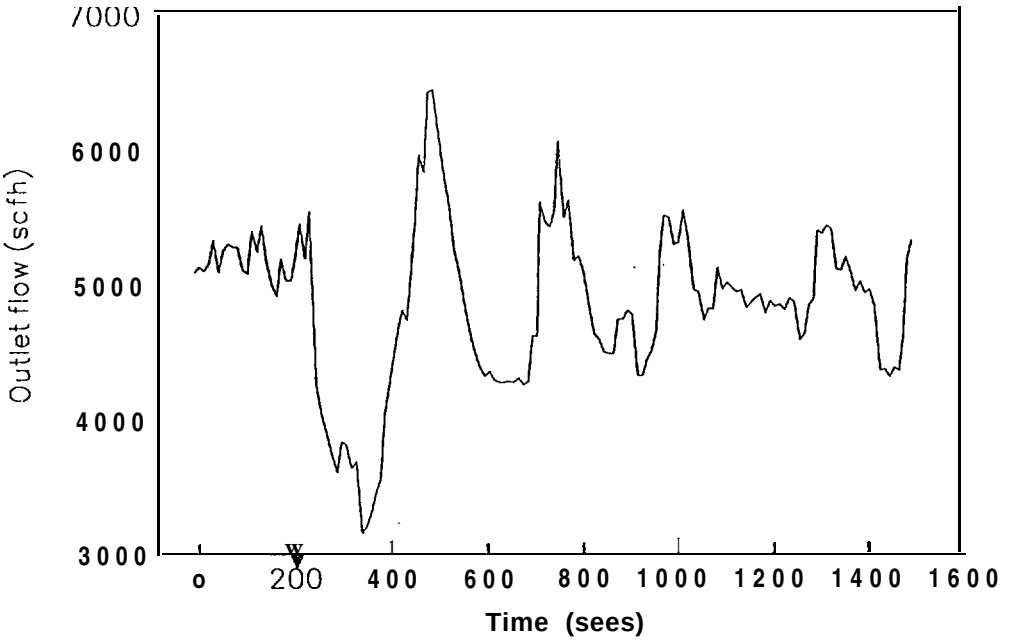

Fig. 4: High order response of Outlet Flow for a change in Reactor Air Flow from 1060 to 940 scfh **(made at time indicated by ▼).**

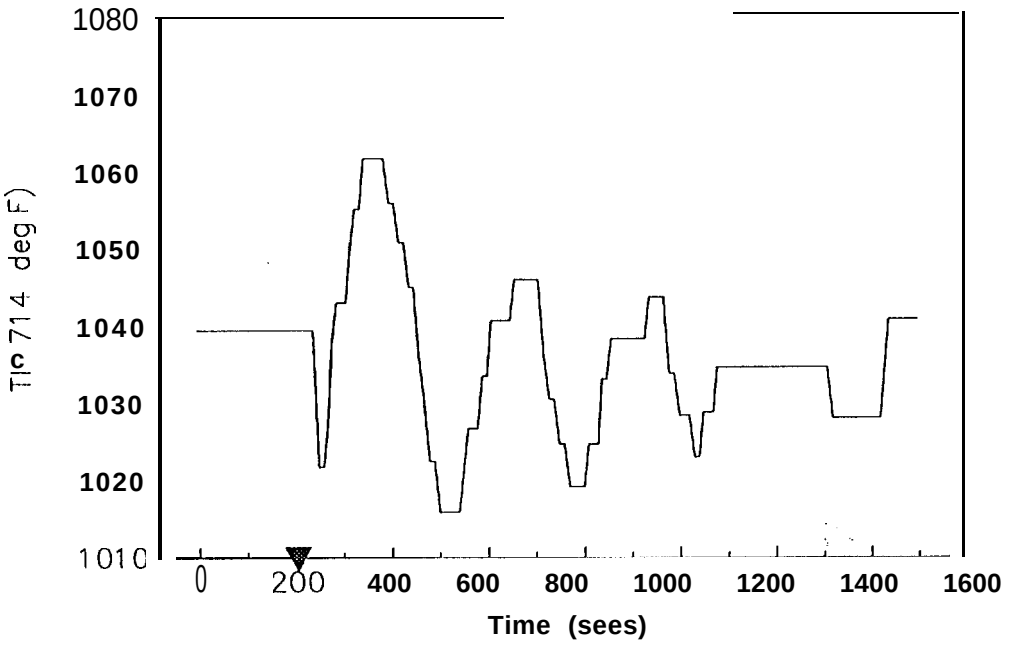

Fig. 5: High Order Response of TIR 714 for a change in Reactor Air Flow from 1060 to 940 scfh (made at time indicated by ▼).

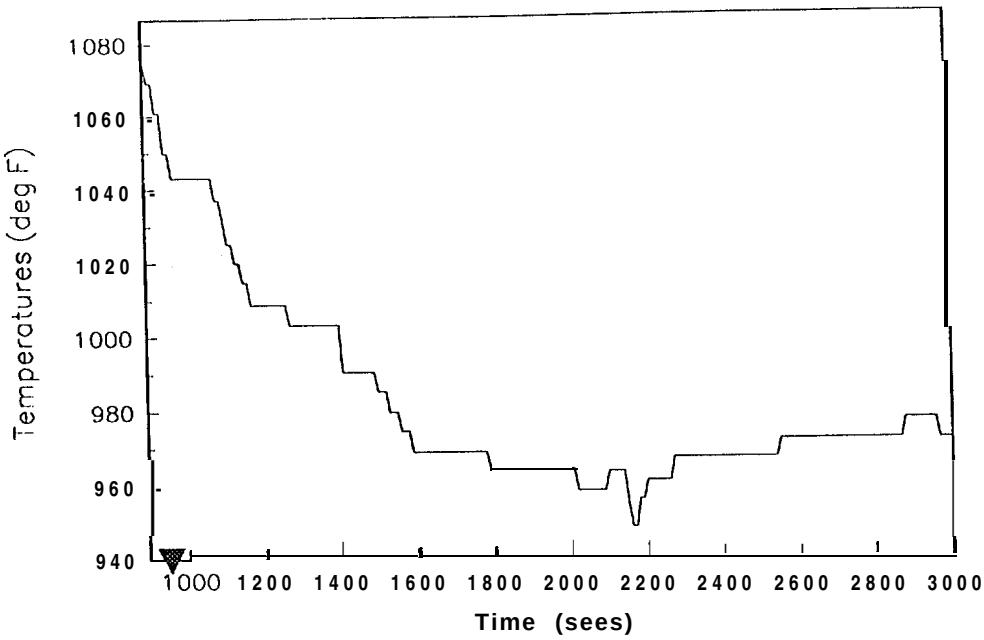

Fig. 6: Response of TIR 700 for a change in Cone N2 from 50 to 100 scfh (made at time indicated by ▼).

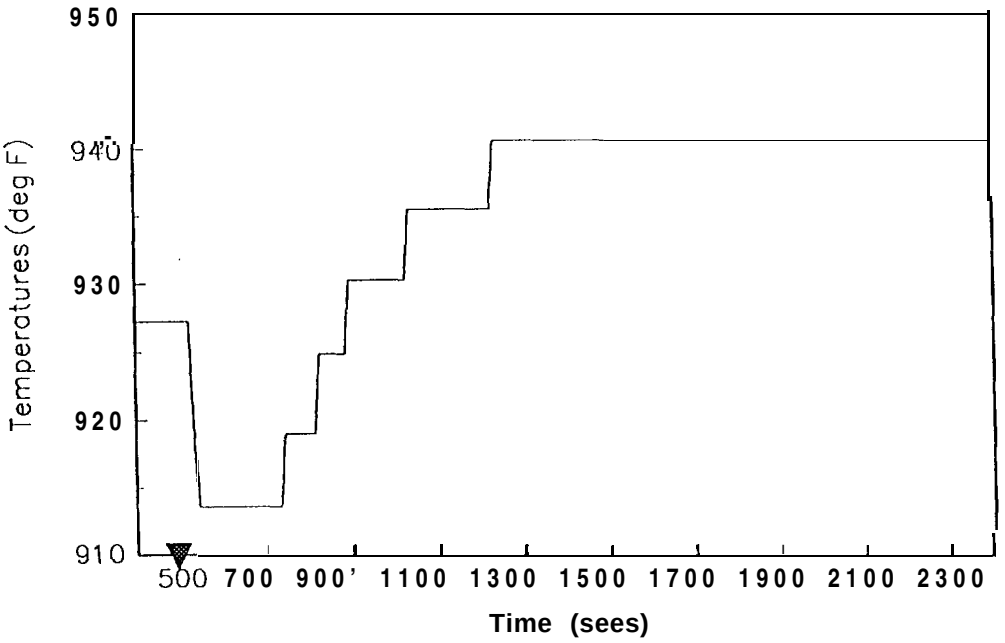

Fig. 7: Inverse Response – TIR 700 for a change in Cone N2 from 150 to 50 scfh (made at time indicated by ▼).

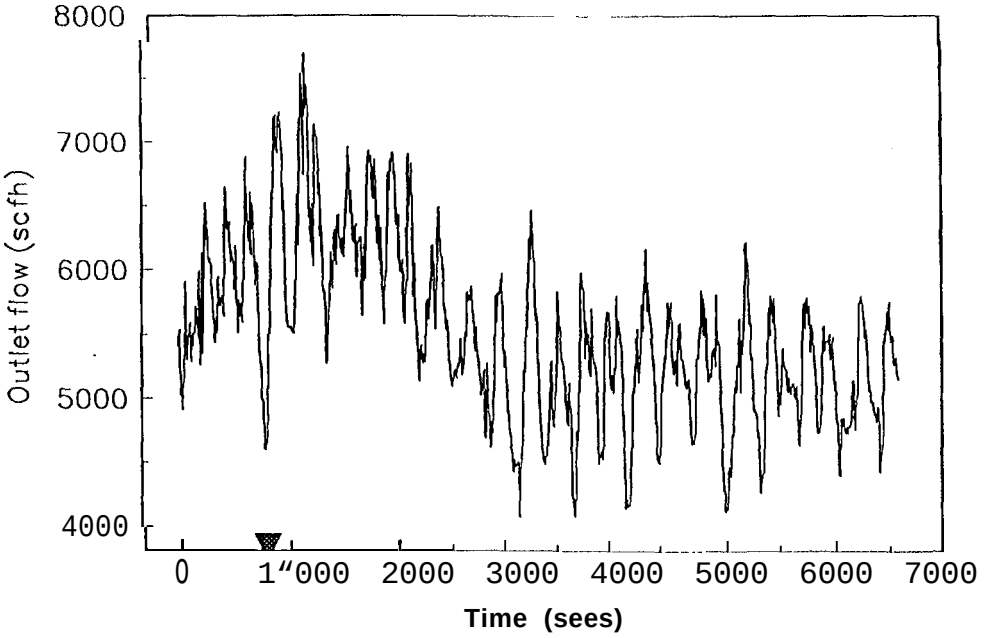

Fig. 8: Noisy Response – Outlet flow rate for a change in *Cone* N2 from 50 to 100 scfh (made at time indicated by ▼).

Transfer Function: $\frac{T_i(s)}{F_{N_2}(S)} = \frac{K e^{-\theta s}}{\tau s + 1}$

	FBG Data			MGAS	
	K	τ	θ	K	τ
TIR 703	-0.0200	500	-	-0.0200	300
TIR 702	0.0805	2000	1000	-0.0220	280
TIR 707	---------	------	-------	-0.0220	50
TIR 701	-0.1051	500	-	-0.0240	75
TIR 700	-0.2421	700	-	-0.0231	100
TIR 704	-0.0504	600	-	-0.0171	200
TIR 705	-0.0298	200	-	-0.0170	120
TIR714	-0.0302	200	-	-0.0160	75

Table 2: Process parameters for the response of Reactor Temperatures for a change in Cone Nitrogen from 50 to 100 scfh.

FBG Data				MGAS						
T.F : $\frac{-P_{i\,(S)}}{F_{N_2\,(S)}}$		$\frac{K e^{-\theta s}}{\tau s + 1}$		Transfer Function: $\frac{P_{i\,(S)}}{F_{N_2}(s)} = \frac{K_1 e^{-\theta_1 s}}{\tau_1 s + 1} + \frac{K_2 e^{-\theta_2 s}}{\tau_2 s + 1}$						
PDIR	K	τ	θ	PDIR	K_1	τ_1	θ_1		K_2	τ_2	θ_2
706	-0.5769	400		706	--	--	--		--	--	--
718	-0.2400	400		718	--	--	--		--	--	--
707	--	--	--	707	0.0501	25			0.0672	875	500
708	--	--	--	708	0.0301	25			0.0341	1375	800
709	--	--	--	709	0.0232	25			0.0285	1800	1150
431	--	--	--	431	0.0217	25			0.0226	2000	1250
710	--	--	--	710	0.0118	25			0.0119	2200	1750

Table 3: Process Parameters for the response of Pressure Differentials for a change in Cone Nitrogen from 50 to 100 scfh.

Compositions:

Transfer Function: $\frac{Y_i(s)}{F_{N_2}(s)} = \frac{K e^{-\theta s}}{\tau s + 1}$

	FBG Data			MGAS		
	K	τ	θ	K	τ	θ
Y_{CO}	-0.04	700	-	-0.0109	25	-
Y_{CO_2}	0.0	--	--	-0.0187	30	-
Y_{H_2O}	0.0	--	--	-0.0040	175	-
Y_{CH_4}	0.0	--	--	-0.0005	25	-
Y_{H_2}	-0.05	400	-	-0.0012	20	-
Y_{H_2S}	0.0	--	--	-0.00002	30	-
Y_{N_2}	0.12	500	-	0.0331	50	-

Outlet flow:

Transfer Function: $\frac{F_g(s)}{F_{N_2}(s)} = \frac{K e^{-\theta s}}{\tau s + 1}$

	FBG Data			MGAS		
	K	τ	θ	K	τ	θ
FGAS	-0.3	1000	-	-0.3	1000	-

Table 4: Process Parameters for the response of Compositions and Outlet Flow for a change in Cone Nitrogen from 50 to 100 scfh.

Transfer Function: $$\frac{T_i(s)}{F_{air}(s)} = \frac{K e^{-\theta s}}{\tau s + 1}$$

	FBG Data			MGAS		
	K	τ	e	K	τ	θ
TIR 703	-0.0918	25	-	0.1860	275	-
TIR 702	0.1764	50	-	0.2481	175	-
TIR 707	-----	-----	-----	0.1760	30	-
TIR 701	0.1736	150	-	0.2114	60	-
TIR 700	0.2206	150	-	0.2214	100	-
TIR 704	0.2205	75	-	0.1584	225	-
TIR 705	0.2643	100	-	0.1148	175	-
TIR 714	0.3663	125	-	0.0968	125	-

Table 5: Process Parameters for the response of Reactor Temperatures for a change in Reactor Air from 1060 to 940 scfh.

Transfer Function: $\frac{P_i(s)}{F_{air}(s)} = \frac{K_1 e^{-\theta_1 s}}{\tau_1 s + 1} + \frac{K_2 e^{-\theta_2 s}}{\tau_2 s + 1}$

	FBG Data						MGAS					
PDIR	K_1	τ_1	θ_1	K_2	τ_2	θ_2	K_1	τ_1	θ_1	K_2	τ_2	θ_2
707	0.1178	50	-	-0.1000	50	20	0.3094	10	-	-0.5890	850	400
708	0.1178	50	-	-0.1200	50	20	0.1913	10	-	-0.4005	1350	750
709	0.2356	50	-	-0.7067	100	50	0.1471	10	-	-0.2944	1750	900
431	-----	---		-----	----	---	0.1177	10	-	-0.3108	2000	1300
710	0.0353	50	-	-0.2356	100	50	0.0442	20	-	-0.0746	2400	1500

Table 6: Process Parameters for the response of Pressure Differentials for a change in Reactor Air from 1060 to 940 scfh.

Compositions:

Transfer Function: $$\frac{Y_i(s)}{F_{air}(s)} = \frac{K e^{-\theta s}}{\tau s + 1}$$

	FBG Data			MGAS		
	K	τ	θ	K	τ	θ
Y_{CO}	0.0873	75		0.0309	75	
Y_{CO_2}	-0.0087	50		0.0175	400	
Y_{H_2O}	------	---	---	-0.0530	75	
Y_{CH_4}	------	---	---	-0.0018	75	
Y_{H_2}	-0.0407	100		------	----	---
Y_{H_2S}	------	---	---	------	----	---
Y_{N_2}	0.0707	300		0.0213	25	

outlet **flow:**

Transfer Function: $$\frac{F_g(s)}{F_{air}(s)} = \frac{K_1 e^{-\theta_1 s}}{\tau_1 s + 1} + \frac{K_2 e^{-\theta_2 s}}{\tau_2 s + 1}$$

	FBG Data						MGAS					
	K_1	τ_1	θ_1	K_2	τ_2	θ_2	K_1	τ_1	θ_1	K_2	τ_2	θ_2
FGAS	3.356	25	-	-3.418	200	75	0.027	10	-	-0.014	200	25

Table 7: Process Parameters for the response of Compositions and Outlet Flow for a change in Reactor Air from 50 to 100 scfh.

VI. Plan of Action

This is a rough updated plan of action for modeling and control of the METC FBG. This plan outlines some of the issues that were discussed during USC's visit to METC on 3/13/95 and suggests actions to be taken to address them. This plan is consistent with the original scope of work in the contract.

1. In this report, we have presented some selected responses meant to show that the gasifier exhibits behavior that is challenging from a control point of view. We have discussed many of these responses with the FBG operations experts at METC to interpret these results. These discussions were very beneficial from our point of' view, and will be factored into later versions of the FBG model.

   We will therefore meet in a small group (comprised of S. Noel, J. Rocky, the engineers and technicians responsible for the FBG, and USC) on a more frequent basis and prior to presenting results in a formal seminar at METC.

2. It is possible that the primary cause of premature shutdown during run #10 was due to a poorly tuned pressure controller which manipulates the exit gas flow. It appears that the controller was overacting to small changes (less than 2 psi) in the gasifier pressure. There is also some uncertainty as to how the pressure control scheme is configured since there are two valves in the loop. It was suggested that a split-range controller may be what is employed,

   We will examine all of the data during (pressure, exit flow, inlet flows, temps) the time period of interest to confirm that the controller was indeed the problem.

The operation of the present pressure control system must be determined (by METC). Once we know what we are dealing with, a general analysis of the control strategy will be made at USC with suggestions for improvements

The control valve(s) manipulating the exit stream should be checked for proper operation. If valves are not working properly, no amount of controller retuning will solve the problem. Once we are certain that there are no hardware problems, the controller can be retuned. This should be done on-line under gasification conditions. A trial retuning should be made during cold start to determine that the controller is acting as expected. Alternatively, one could put the pressure controller in 'manual'. However, this will pose other problems for those actually running the gasifier.

In addition, we will supply references on applied controller tuning and on split-range controllers. We will also send PICLES, a simple controller tuning simulator which will run on a PC.

3. The data from gasifier runs 8,9, and 10 can all be used to develop a simple gasifier model. The main problem in using all of this data is that the data is spread over a wide range of operating conditions. The initial control modeling plan was to develop a linear model based on small perturbations from a single operating condition (during run #l O). A linear model is generally valid only near the operating conditions for which it is developed.

We will examine the extent of nonlinear behavior exhibited by the gasifier (using data from runs 8,9, and 10). If it is nonlinear as expected, we can train a neural network model from the steady state data. This model can be used to examine the control at a given operating point and also to find an optimal operating condition (within the

envelope of conditions in the process data, i.e.- it won't extrapolate). The accuracy of the neural network model will depend upon the richness of the data from runs 8,9 and 10.

Note that neural network modeling was part of our contract already. This path will be pursued in parallel with the linear transfer function modeling presently underway.

4. Larry Lawson is putting together a control relevant model of PYGAS using TUTSIM. We would like to stay updated on that work as it appears to be the beginnings of a useful model for control purposes. We would even like to obtain a copy of the model at various stages in its development,

5. As for the present Transfer Function modeling:
   S. Reddy will check the present model (there appeared to be some inconsistencies). Appropriate data from the May gasifier run will be added to this model. We will load and run the GQjet spreadsheet model and compare the gains with the transfer function model and also the neural network model. He will also continue with MGAS, adjusting some model parameters and adding a recirculation loop in an attempt to obtain better agreement with the data. Of particular interest is the large discrepancy between the actual time constant and that predicted by MGAS.

6. The success of the modeling and control studies depends upon coupling the process data with the expertise and experience of those running the gasifier. The process data does not always tell the real story. So much is going on during the gasifier run that an important event may be completely missed by simply looking at the sensor data.

We will look more closely at the daily log sheets. More importantly, we will keep in contact (on a weekly basis) with the FBG group. Modeling results will be presented more frequently. This should promote a more frequent exchange of information and ideas.